A Power Limiting Control Strategy Based on Adaptive Utility Function for Fast Demand Response of Buildings in Smart Grids

Rui Tang, PhD student, is a PhD student in the Department of Building Services Engineering, The Hong Kong Polytechnic University, Kowloon, Hong Kong.

Shengwei Wang, PhD, CEng, MASHRAE, is a chair professor in the Department of Building Services Engineering, The Hong Kong Polytechnic University, Kowloon, Hong Kong.

Dian-ce Gao, PhD, is a research fellow in the Department of Building Services Engineering, The Hong Kong Polytechnic University, Kowloon, Hong Kong.

Kui Shan, PhD, is a post-doctoral fellow in the Department of Building Services Engineering, The Hong Kong Polytechnic University, Kowloon, Hong Kong.

Abstract: Power imbalance in electrical grid operation has become a most critical issue that results in a series of problems to grids and end-users. The end-users at demand side can actually take full advantage of their power reduction potentials to alleviate the power imbalance of an electrical grid. Buildings, as the major energy end-users, could play an important role on power demand response in smart grids. This paper presents a fast power demand limiting control strategy in response to the sudden pricing changes or urgent requests of grids within a very short time, i.e. minutes. The basic idea is to shut down some of active chillers during demand response (DR) events for immediate power demand reduction. The paper focuses on the solutions to address the operation problems caused by the conventional control

logics, particularly the disordered flow distribution in chilled water system. A water flow supervisor based on an adaptive utility function is developed for updating the chilled water flow set-point of every individual zone online. The objective is to maintain even indoor air temperature change among all zones during a DR period. A case study is conducted in a simulation platform to test and validate the novel control strategy. Test results show that the proposed control strategy can achieve fast power reduction after receiving a demand response request. Simultaneously, the proposed control strategy can effectively solve the problem of disordered water distribution and achieve the similar changing profiles of the thermal comfort among different zones under the reduced cooling supply.

Key words: fast demand response, adaptive utility function, air-conditioning control, demand limiting, smart grid.

Introduction

The world is facing great challenges from the depletion of fossil fuels, dramatic growth of energy demand and global climate change. The increasing use of renewable energies is a logical response to those challenges. However, the integration of large amounts of renewable generations, whose capacities heavily depend on weather conditions (e.g. solar density, wind speed), would cause significant stress on the balance of electricity grids (IEA 2014; Hirst 2001). Any significant imbalance might cause grid instability or severe voltage fluctuations and even grid failures. Large scale power outages have frequently occurred in recent years worldwide, such as the Indian blackout (2012), Brazil blackout (2009), Northeast blackout in the United States (2003), Italy blackout (2003).

Smart grid technology provides a promising solution for enhancing the balance of power grids by improving the ability of electricity producers and consumers to communicate with each other and make decisions about how and when to produce and consume electrical power (Yuan and Hu 2011). The suppliers are expected to increase the price to discourage power use at times of peak demand so as to reduce

generation costs or to avoid grid failures. Consumers would benefit from cost savings if they voluntarily alter or reduce the level of instantaneous demand, known as demand response (DR). As one of the most important means in the electrical grid management, DR has become an essential action or control taken by the end-users to change their load profiles under a specified pricing policy or request of the grid, which are dynamic or event-driven short-term modifications.

Buildings, as the primary energy end-users, could play an important role on power demand response in smart grids. Buildings consume about 40% of the U.S. primary energy consumption, 73.6% of all electricity in the United States (DOE 2012) and over 90% in Hong Kong (EMSD 2012). In fact, individual buildings are capable of interacting with smart grids due to the popular use of building automation systems and the advanced smart meters. At the same time, the interaction between buildings and the power grids could be very effective due to elastic nature of building energy use (Wang et al. 2014). The building demand management for demand response aims at minimizing the impact of peak demand charges and time-of-use rates on the service quality of buildings. The HVAC system is an excellent demand response resource as the consumption of HVAC systems accounts for the largest part in buildings (EMSD 2012) as well as their elastic nature. Demand shifting and demand limiting are the two major means for peak demand management.

Demand shifting in buildings is the process of shifting on-peak load to off-peak hours so as to take advantage of electricity rate difference in different periods. With the thermal energy storage (TES) systems, thermal energy can be provided and stored in the night and then released to the indoor environment during the day (Fukai et al. 2003; Ousksou et al. 2010； Cui et al. 2014). Many efforts have been made to enhance TES systems. Some of the available researches focused on improving heat transfer efficiency (Kenisarin and Mahkamov 2007; Sharma et al. 2009; Demirbas 2006; Hamdan 2004). While some other researches focused on phase change material (PCM) for thermal storage (Bal et al. 2010; Tyagi et al. 2011; Oya et al. 2012; Ling and Poon 2013; Bentz and Turpin 2007; de Gracia et al. 2013).

Demand limiting is the practice of restricting the peak power demand of a building in such a way that the total power does not exceed the pre-defined peak demand during periods of time where power is at a premium cost. Lee and Braun (2008) proposed three simple approaches for estimating building zone temperature set-point variations that minimize peak demand during critical demand periods and evaluated the peak load reduction potential associated with implementation of these methods. Sun et al. (2010) conducted case studies concerning on the peak demand reduction to compromise energy cost and peak demand charge using indoor air temperature set-point reset strategy. The indoor air temperature set-point reset strategy allowed significant power reduction of HVAC systems during the peak hours. Xu and Haves (2006) conducted a preliminary case study to demonstrate the potential of utilizing building thermal mass for peak demand reduction in an office building in California. Two precooling and zone temperature reset strategies were tested. The results showed that a simple demand-limiting strategy could reduce the chiller power significantly.

In smart grids, users could be informed of pricing changes or DR requests one day ahead, hours ahead or even minutes ahead depending on the prediction accuracy and the degree of emergency. When pricing changes are informed hours ahead, rescheduling the system operation, such as resetting the indoor air temperature, is a preferable alternative to reducing the power demand of air-conditioning systems. When adding additional generation capacity is extremely expensive or at times of supply shortage, sudden pricing changes or urgent incentives are necessary alternatives to achieve the demand reduction within a very short time, i.e. minutes. In such a case, conventional building demand management strategies would not be sufficient to fulfill the needs of the grid real time operation.

In fact, shutting down some of the chillers can achieve immediate demand reduction (Xue et al. 2015). However, simply shutting down chillers at the cooling supply side of an air-conditioning system will result in disorder of the entire air-conditioning system control and uneven reductions of cooling supply among the

air-conditioned spaces. This is because almost all the conventional control strategies used today for centralized air-conditioning systems are “demand-based” feedback control strategies, which mean the cooling supply by chillers is set to be enough to fully satisfy the requirements of the terminal units (e.g., air-handling units). But in the cases of supply limiting, all cooling demand side users will compete for the limited cooling supply. The reductions among users will not be even and the indoor environment in some zones will be sacrificed to unacceptable levels much more quickly. Therefore, new building demand management and control strategies are essential to cope with sudden cooling supply capacity limitations if commercial buildings are to achieve fast power demand reduction in response to short-term pricing changes or urgent requests from smart grids for demand reduction.

This paper, therefore, proposes a fast demand response and power limiting control strategy by limiting cooling supply allowing the commercial buildings to actively and effectively respond to short-term pricing changes/urgent requests from smart grids. Models are developed for online control aiming to avoid the serious problem of the uneven thermal comfort sacrifice among different zones, which will happen usually when using the control strategies commonly used today.

A new power limiting control strategy based on an adaptive utility function is developed to reset the chilled water flow set-points of individual zones online, which are reduced proportionally to the cooling demands. The method could maintain even indoor air temperature changes among all zones and avoid the increase of pump power during a DR period.

Commonly-used control strategies and associated problems in demand limiting control

Almost all the automatic control strategies used for air-conditioning systems in buildings today are demand-based feedback control strategies. To illustrate the philosophy of the control response of the changes of cooling loads of different zones in a building, a typical control strategy commonly used today is selected here. Figure

1 shows the schematic of the control strategy for a primary constant-secondary variable chilled water system. The water valve opening of individual air handling unit (AHU) is modulated to maintain the supply air temperature at the preset set-point. For the speed control of the secondary chilled water pumps, their speed will be adjusted to ensure the measured pressure drop of the main supply side (or the remote critical loop) at its set-point. The chiller sequence/capacity will be properly controlled to meet the cooling load required.

However, during DR period, serious operation problems would occur if simply shutting down some of the chillers (without any other measures) under this control strategy. In this case, the cooling capacity provided by operating chillers is limited and could not fully meet the requirement of the AHUs at the cooling demand side. All demand side users will compete for the limited cooling supply. The chilled water distributed among users will not be even (or not proportional to their needs), which could result in the fact that the indoor environments in some zones will be sacrificed to unacceptable level much more quickly than other zones. In addition, some other extremely serious operation problems would also be caused. For instance, secondary chilled water pumps would be over-speeded due to the need to maintain the preset differential pressure in the condition of fully opened valves, which would lead to significantly increased pump power.

Figure 1. Outline of a typical chilled water system control strategy used today

A case study was conducted on a simulated chilled water platform by TRNSYS to illustrate the operation problems when using the above control strategy during DR event. The chilled water system for a commercial building consists of six chillers, two secondary water pumps and six groups of AHUs, having the same configuration as shown in Figure 1. Six identical zones with the same cooling load profile served by the six identical AHUs from each group were selected. In a typical working day, the

DR event was set between 15:00pm and 17:00pm, during which two of the four active chillers were shut down.

Figure 2 shows the chilled water flow rates and indoor air temperatures of the six zones. It can be found that, before and after a DR event, the chilled water flow rates and the indoor air temperatures of all zones were almost the same. However, during the DR event, the chilled water distribution was extremely unbalanced. The total chilled water distributed to all zones increased significantly due to facts that the valves of AHUs were fully open to compete for the limited cooling supply after some of the operating chillers were shut down during the DR event, as illustrated in Figure 3. The nearest zone (Zone 6) obtained the highest water flow, while the most remote zone (Zone 1) obtained the least water flow. This is because the valves of all AHUs were fully opened to compete for more water flow due to the fact that their supply air temperatures could not be maintained at the set-points when the cooling supply by chillers was reduced. Consequently, the indoor air temperature rises of individual zones would be uneven (indoor air temperature set-points of all zones are 24℃), as shown in Figure 2(b). The indoor air temperature of the zone with least flow would reach 26℃ and the largest temperature difference among zones was about 1.5℃.

Figure 2. Water distribution and indoor air temperature profiles of a DR test using conventional control strategy

Another problem concerning the pump operation is shown in Figure 3. In normal conditions, the water flow rate in bypass line was positive, which means that the flow rate of the primary loop was more than that of the secondary loop. However, serious negative water flow, namely deficit flow, was observed during DR event. During DR event, the flow rate of the secondary loop was more than that of the primary loop. The occurrence of deficit flow means excessive water flow was circulated by the secondary pumps. Consequently, both secondary pumps were running at their full

speed (i.e., 50HZ) during DR event. Extra pump power was consumed, which in fact reduced the effect of power reduction of DR control.

Figure 3. Water flow rate in bypass line and secondary pump power of a DR test using conventional control strategy

Concept of utility value and development of adaptive utility function

"Utility" is an important concept in economics and game theory, which represents satisfaction experienced by the consumer of a good. Utility function expresses utility as a function of the amounts of the various goods consumed, which establishes the relationship between goods consumed and people's satisfaction (Varian 1992). This concept has been used in many other areas, besides economics. For example, utility function has been widely used in wireless resource management, such as bandwidth allocation (Kuo and Liao 2007; Kalyanasundaram 2002).

The problem concerned in this study is very similar to the utility concept in economics. An adaptive utility function is proposed to solve the problem concerning water flow distribution. The chilled water is the allocation resource, while the indoor thermal comfort in terms of the indoor air temperature is chosen as the utility value after normalization.

Definition of utility value

In this study, the case studies of demand response control are conducted in cooling conditions. The utility value (U_i) of i^{th} zone can be defined as Eq.(1), which represents the degree of the satisfaction on the indoor thermal comfort.

$$U_i = 1 - \frac{|T_i - T_{set,i}|}{T_{band}} \qquad U_i \in [0,1] \tag{1}$$

where, T_i is the measured indoor air temperature of i^{th} zone. $T_{set,i}$ is the reference set-point (e.g. 24°C in this study) of indoor air temperature which is originally

predefined during normal period. T_{band} is the maximum deviation between T_i and $T_{set,i}$, which is chosen as 10°C in this study. This value is selected to be large enough, i.e. clearly larger than the value needed to cover all the possible temperature range that might be considered practically in DR events, including extreme cases of very large temperature rise in DR events. According to Eq.(1), a higher indoor air temperature means a lower utility value (i.e. less satisfaction). When T_i equals to $T_{set,i}$, the utility value is 1, which means the best satisfaction. When the measured indoor air temperature is 10°C higher than the reference set-point, the utility value becomes zero (i.e., the least satisfaction).

Adaptive utility function correlating indoor air temperature and water flow rate

The utility value (U_i) in Eq.(1) is defined as an index which represents the indoor air temperature in this study. The utility value is assumed as a function of the chilled water flow rate. In fact, the indoor air temperature is also affected by a few other factors, such as the supply air temperature and cooling load. However, during a very short time interval, those factors can be considered unchanged and the correlation function (i.e., utility function) of fixed parameters between the indoor air temperature and chilled water flow rate is valid. To allow the use of the utility function over the entire working range during a DR event, one of the two parameters of the utility function is updated online and the adaptive utility function is employed as explained later.

In this paper, a quadratic function is chosen as the form of the utility function, correlating the chilled water flow rate ($M_{w,i}$) supplied to each individual zone, as shown in Eq.(2). The selection of the utility function form and the procedure of parameter identification are shown in next session. It can be found that the utility value will reach 1 if $M_{w,i}$ is equal to $M_{U=1,i}$, which means that the indoor air temperature is maintained at its set-point. If $M_{w,i}$ is less than $M_{U=1,i}$, the utility value

will be less than 1, which means that the indoor air temperature is higher than its set-point.

$$U_i = -a_i(M_{w,i} - M_{U=1,i})^2 + 1, \qquad M_{w,i} < M_{U=1,i} \tag{2}$$

where, $M_{w,i}$ is the water flow rate supplied to i^{th} zone. $M_{U=1,i}$ is a fictitious reference value of the water flow rate which is required to maintain the indoor air temperature at its original set-point before DR event but under current cooling load condition. a_i is a parameter representing the thermodynamic characteristics of the zone. Generally, the parameter, a, of a zone with higher cooling load, that requires more chilled water flow, would be relative small and it would be less sensitive to the unit change of the chilled water flow.

Formulation of the adaptive utility function

In order to select a proper formula correlating the indoor air temperature (i.e., utility value) and the chilled water flow rate of each zone, case studies were carried out under the simulation platform developed on TRNSYS. The studied chilled water system consists of 6 AHUs, each serving one zone. At a constant supply water temperature (i.e., 7°C), the change of the indoor air temperature was obtained when the supply water flow rate was changed. During the test, the air flow rate of each AHU was set to be constant and the cooling load of each zone was constant. All six zones were studied and only one zone was selected here for illustration. Figure 4(a) shows the relationship between indoor air temperature and the chilled water flow rate. Figure 4(b) illustrates the relationship between the water flow rate and the utility value calculated based on the measured indoor air temperature. It can be observed that there is roughly a quadric relation between the utility value and the supply chilled water flow rate of each zone.

Figure 4. Utility value *vs* chilled water flow rate

In the utility function (Eq.(2)), parameter $M_{U=1,i}$ is the required water flow rate to maintain the indoor air temperate of each zone at its set-point, which actually varies according to the cooling load conditions. If the current indoor air temperature is maintained at its set-point, $M_{U=1,i}$ is equal to the current water flow rate. During DR event when the actual indoor air temperature of a zone is higher than its set-point, $M_{U=1,i}$ is then the expected or fictitious value and it is larger than the current water flow rate. The adaptive method is used for updating $M_{U=1,i}$ online following the change of load condition in this study.

It is worth of noticing that parameter a_i is also a variable depending on the cooling load conditions for certain zone. However, even a_i varies in a range, it has no significant impact on the calculation of the supply water flow rate set-point during DR event, thanks to the way of using the adaptive utility function and the updating of the other parameter, $M_{U=1,i}$. Therefore, constant values but different for different zones are predefined in this study. The process of identifying the parameter a is introduced in the section "test platform".

Online parameter updating of the adaptive utility function and water flow set-point prediction

The parameter, $M_{U=1,i}$, in the utility function as shown in Eq.(2), is assumed to be a constant within a small range of working condition and a short time interval, but it is regarded as a slowly-varying coefficient, allowing the function to be an adaptive utility function. The value of this parameter at current time step k is determined by the current water flow rate and utility value as shown in Eq.(3). A filter is adopted to fulfil the need of practical in-situ applications of the control strategy, while the measurements always have obvious noise and fluctuation. Before the measurements are used by the strategy, the simple data filter using a forgetting factor is applied to the updated $M_{U=1,i}$ as shown in Eq.(4). Where, λ is the forgetting factor selected to be 0.95 in this study.

$$M_{U=1,i}^{k} = M_{w,i}^{k} + \sqrt{\frac{1-U_i^k}{a_i}} \tag{3}$$

$$M_{U=1,i}^{k} = \lambda M_{U=1,i}^{k-1} + (1-\lambda) M_{U=1,i}^{k} \tag{4}$$

Having the updated $M_{U=1,i}^{k}$, the utility function can be used to estimate the water flow rate needed to achieve any target utility value for a zone after rewriting, as shown in Eq.(5).

$$M_{sp,i}^{k} = M_{U=1,i}^{k} - \sqrt{\frac{1-\bar{U}_{sp}^{k}}{a_i}} \tag{5}$$

where, $\bar{U}_{sp}^{k}$ is the target utility value of all zones at current time step, which is the expected utility value of all zones if the temperatures (utility values) of all zones are controlled to be the same and the available cooling capacity is fully used.

Proposed fast demand response and power limiting control strategy

Overall structure of the control strategy

In this study, a fast demand response and power limiting control strategy is developed by intentionally shutting down some of active chillers during the DR event while providing the solutions to the inherent operation problems of commonly used control strategies. It is noted that this paper focuses on developing a chilled water flow distribution scheme to address the improper chilled water distribution among each zone under insufficient cooling supply during DR event. The problem concerning how to determine the number of chillers to be shut down is not discussed in this paper.

As shown in Figure 5, the chilled water flow distribution scheme employs a supervisor (namely water flow distributor) to continuously adjust the set-points of chilled water flow rates of individual zones. At each time step, the set-points are reset aiming at maintaining the same indoor air temperature rise, i.e. the same utility value,

among different zones, as illustrated by Eq.(6). At the same time, the constraint given by Eq.(7) should be satisfied in order to prevent the water flow rate of the secondary loop exceeding that of the primary loop. For each group of AHUs, a feedback (PID) control is employed. With the given set-point from the water flow supervisor, the PID controller controls the water flow rate of the AHU at the set-point by modulating the flow control valve. The major work of this study is to develop the water flow distributor, which is described in detail as follows.

Figure 5. Proposed chilled water flow control strategy

$$\sum_{i=1}^{n}(U_i - \bar{U}_i)^2 = 0 \tag{6}$$

$$|\sum_{i=1}^{n} M_{sp,i} - M_{w,tot}| < \varepsilon \tag{7}$$

where, U_i is the utility value of i^{th} zone at a time step. $\bar{U}_i$ is the average utility of all zones. n is the total number of zones. $M_{sp,i}$ is the chilled water flow set-point of i^{th} zone at current time step. $M_{w,tot}$ is the total available chilled water flow in primary loop. ε is a preset threshold.

Water flow distributor based on adaptive utility function

In this study, the major problem involved in the water flow distributor is how to properly distribute the chilled water among different zones so as to have similar satisfactions/sacrifices of thermal comfort in all zones when the cooling supply from the chiller plant is limited.

Figure 6 shows the flow chart for online water flow rate set-point reset scheme in the water flow distributor. First, the current state variables of each zone, such as the indoor air temperature (T_i^k) and the water flow rate provided ($M_{w,i}^k$), are collected. Then, the utility value (U_i^k) of each zone is calculated based on the definition (Eq.(1)).

After that, the parameter ($M^k_{U=1,i}$) of utility function for each zone is updated online using the current utility value and actual water flow rate (Eq.(3)), followed by a filter for each zone. The average value ($\bar{U}^k$) of the actual utility values (U^k_i) of all zones is used as the initial target value for all zones and the water flow rate set-point ($M^k_{sp,i}$) of each zone is determined using the updated utility function (Eq.(5)), which correlating the utility value and water flow rate. Finally, a flow limit check and fine-tune scheme is employed to check whether the sum of the target water flow rate set-points ($\sum M^k_{sp,i}$) is equal to the actual total water flow rate of the primary loop ($M^k_{w,tot}$). This ensures the even temperature rise in all zones, and at the same time, avoids the deficit flow also and fully uses the limited cooling supply. If the $\sum M^k_{sp,i}$ is no equal to $M^k_{w,tot}$, the target utility value ($\bar{U}^k_{sp}$) will be fine-tuned with a predefined incremental (Δu). The updated target utility value is then used to calculate of the water flow set-points again until the difference between the total flow set-point and the actual total flow rate is within a preset threshold. The final water flow rate set-point ($M^k_{sp,i}$) of each zone is then set as the set-point for the flow control of the AHU.

Figure 6. Flow chart for online water flow set-point reset scheme

Test platform

Setup of test platform

Computer-based dynamic simulation is adopted, as an effective mean, to test and validate the online control strategies (Wang 1998). In this study, a virtual test platform is built to test the proposed fast demand response and power limiting control strategy using dynamic models developed on TRNSYS. This test platform employs detailed physical models including the building envelop and major components (e.g. chillers, pumps, hydraulic network, AHUs) of a central air-conditioning system. The dynamic

processes of heat transfer, hydraulic characteristics, flow balance, energy conservation and controls among the whole system are simulated. The weather data adopted is a typical summer day in Hong Kong, as shown in Figure 7. The original indoor air temperature set-point before DR event is 24°C. The office time of the building is between 08:00am and 18:00pm. The DR period is between 15:00pm and 17:00pm.

The simulated central chiller plant is a typical primary constant-secondary variable chilled water system. It consists of six identical chillers with rated capacity of 4080 kW. Each chiller is associated with a primary chilled water pump of constant speed (172.5 L/s) and a condenser cooling water pump of constant speed (205 L/s). Six air-conditioned zones in a commercial building have different sizes and different cooling load profiles. The areas of the six zones are 1600 m^2, 1600 m^2, 1600 m^2, 2400 m^2, 1200 m^2, 1600 m^2 respectively. The ceiling height of each zone is 3.5m. The window-to-wall ratio is 0.5.

In the test, there are four operating chillers before the start of DR event, and two of the operating chillers are shut down and two chillers remain to operate.

Figure 7. Weather condition of the test day

Identification of parameter *a*

In Eq.(2), parameter *a* for each zone should be identified before application. *a* is a varying coefficient representing the thermodynamic behavior of each zone. Theoretically, *a* varies according to the changes of cooling load conditions. Simulation studies are carried out to study the range of *a* under different cooling load conditions for each zone. 20 test cases of one hour DR period are selected including the morning and afternoon sessions of five weekdays in two seasons (2x5x2). The cooling loads of zones during a test case can be assumed to be roughly constant. .

Figure 8 shows the method of identifying parameter *a*. For the thermal zone, a period of one hour with relatively small fluctuation in the cooling load is selected for

the DR test. During the test, the cooling supply from chillers is reduced. The water flow rate before the DR event is regarded as $M_{U=1}$ during DR period assuming the cooling load remains constant during this period. The indoor air temperature gradually increases and reaches a new steady level, from A to B as shown in Figure 8. The chilled water flow rate and the utility value (corresponding to the indoor air temperature at the new steady level) are selected as the values of variables M_w and U and the parameter a of the utility function is then determined by Eq.(8).

$$a = \frac{1-U}{(M_w - M_{U=1})^2} \tag{8}$$

Table 1 shows the values of parameter a for Zone 1 in 20 tests over 10 days. The variation range of a for Zone 1 is between 0.023 and 0.045 under different cooling load conditions. The variation range of a for other zones are presented in Table 2.

Figure 8. The method of identifying parameter a

Table 1 The results of parameter a

Table 2 The results of parameter a of six zones

Based on the variation range of parameter a of each zone, different values are selected to study the impact on the performance of the proposed control strategy. Two case studies are conducted as shown in Table 3. Parameter a of Zone 1 is assigned with two different values (i.e. maximum and minimum). Parameters a of other zones are set to be their own average values, respectively. One typical summer day in Hong Kong is selected for the tests. The demand response period is set to be 2 hours from 15:00pm to 17:00pm in the tests. The proposed control strategy is activated during DR event.

Table 3 The selected values of parameter a

The results of the two case studies are shown in Figure 9. It can be observed that, in both case 1 and case 2, the indoor air temperatures of the six zones almost experienced the same variation and always kept consistent during DR event. This means that the control strategy is not sensitive to the value of parameter a due to the use of adaptive utility function and the updating of parameter $M_{U=1}$. Therefore, in this study, the average value of parameter a of each zone is selected for the following performance evaluation tests of the control strategy.

Figure 9. Indoor temperature profiles of two case studies using different values of a

Results and Discussions

The proposed control strategy was tested in the simulation platform involving six zones. Figure 10 shows the indoor air temperature profiles of the six zones using conventional control and proposed control strategies. In Figure 10(a), the indoor air temperature profiles of the six zones are obviously different not only during DR event, but also right after DR event. This is mainly because the cooling demand are very high and individual zones compete for the chilled water again to push their comfort levels to their set-points right after DR event. Using the proposed control strategy, it can be observed that the temperature profiles of the six zones are almost the same during DR event when the cooling supply from chillers is limited and have a similar resume speed to their original set-points after DR event, as shown in Figure 10(b). Figure 11 presents the actual water flow rates distributed to individual zones using conventional control and proposed control strategies. During and right after DR event, stable and proper chilled water distribution among zones was realized to avoid the disordered water flow distribution (as shown in Figure 11(a)) and maintain the same indoor air temperature change profile of each zone, as shown in Figure 11(b). Figure 12 shows the water flows in the bypass line using the conventional control and the proposed control methods. The proposed control strategies could eliminate the deficit flow and keep the water flow rate in bypass line about zero during DR period.

Figure 10. Indoor air temperature profiles of zones in DR tests using conventional control strategy and proposed strategy

Figure 11. Water flow profiles of zones in DR tests using conventional control strategy and proposed strategy

Figure 13 compares the power consumptions when using the two control strategies, including the electricity use of the primary/secondary chilled water pumps and the chillers. During DR event, the proposed control strategy achieved a power reduction about 1350 kW, accounting for 39% of the power before the start of DR event. Compared with the conventional control strategy, the power is further reduced by about 380 kW (11.2%) using the proposed control strategy mainly due to the power reduction of the secondary pumps. The energy savings during DR event is about 760 kWh (15.3%) using the proposed control strategy.

Figure 12. Water flow rates in bypass line profiles in DR tests using conventional control strategy and proposed strategy

Figure 13. Power consumptions of chillers and chilled water pumps in DR tests using conventional control strategy and proposed strategy

It is worth of noticing that an obvious rebound phenomenon can be observed after DR event when conventional power limiting strategy is used as shown in Figure 13. It reflects the operation when the proposed control is released right after the DR event and the conventional control strategy is resumed. The cooling demand will be very high and individual zones will compete for the chilled water again to push their comfort levels to their set-points. This will lead to very high power demand and unbalanced chilled water distribution. To avoid these problems, the proposed power limiting control strategy is set to continue for a period (e.g., one hour) to guarantee the indoor air temperatures of all zones reaching their original set-points again after DR

period. Besides, the number of chillers (i.e., four) to be activated is the same as that right before the DR event, instead of all chillers. That will also significantly reduce the level of power rebound about 2100KW and effectively avoid the indoor air temperatures of each zone decreasing much lower than their original set-points after DR event. Indoor air temperature of each zone, therefore, will reach their original set-point much more quickly than that using conventional control strategy after DR period.

Conclusions

A novel fast demand response and power limiting control strategy is developed which achieves quick power reduction by properly shutting down some of the chillers. A water flow distributor based on an adaptive utility function is developed to properly distribute the chilled water among different zones to maintain uniform thermal comfort sacrifices during a DR event.

Test results show that the proposed control strategy can achieve fast power reduction when receiving the demand response request. Simultaneously, the proposed control strategy can effectively solve the disordered water distribution problem and achieve the uniform changing profiles of the thermal comfort among different zones under the limited cooling supply. The deficit flow problem also can be avoided. Compared with the conventional control strategy, the power demand is further reduced by about 380 kW (11.2%) during DR event mainly due to the power reduction of the secondary pumps and the energy savings is about 760 kWh (15.3%) using the proposed control strategy. Furthermore, the use of the proposed strategy reduced the level of the power rebound significantly after the DR event.

Acknowledgements

The research presented in this paper is financially supported by a grant (152152/15E) of the Research Grant Council (RGC) of the Hong Kong SAR.

Nomenclature

U = utility value

M = flow

T = temperature

Subscripts

sp = set-point

tot = total

w = water

References

Bal, L.M., S. Satya, and S.N. Naik. 2010. Solar dryer with thermal energy storage systems for drying agricultural food products: a review. *Renewable and Sustainable Energy Reviews* 14:2298–2314.

Bentz, D.P., and R. Turpin. 2007. Potential applications of phase change materials in concrete technology. *Cement and Concrete Composites* 29:527–532.

Cui, B.R., S.W. Wang, C.C. Yan, and X. Xue. 2014. Evaluation of a fast power demand response strategy using active and passive building cold storages for smart grid applications. *Energy Conversion and Management* 102: 227-238.

de Gracia, A., L. Navarro, A. Castell, Á. Ruiz-Pardo, S. Álvarez, and L.F. Cabez. 2013. Thermal analysis of a ventilated facade with PCM for cooling applications. *Energy and Buildings* 65:508–515.

Demirbas, M.F. 2006. Thermal energy storage and phase change materials: an overview. *Energy Sources, Part B: Economics, Planning and Policy* 1:85–95.

DOE. 2012. Buildings Energy Data Book. U.S.: Office of Energy Efficiency and Renewable Energy, Department of Energy.

Electrical and Mechanical Services Department of Hong Kong. 2012. Hong Kong Energy End-use Data. www.emsd.gov.hk/emsd/e_download/pee/HKEEUD_2012.pdf.

Fukai J., Y. Hamada, Y. Morozumi, and O. Miyatake. 2003. Improvement of thermal characteristics of latent heat thermal energy storage units using carbon-fiber brushes: experiments and modeling. *International Journal of Heat and Mass Transfer* 46:4513–4525.

Hamdan, M.A., and I. Al-Hinti. 2004. Analysis of heat transfer during the melting of a phase-change material. *Applied Thermal Engineering* 24:1935–1944.

Hirst, E. 2001. *Real-time balancing operations and markets: key to competitive wholesale electricity markets.* Washington, DC: Edison Electric Institute and Project for Sustainable FERC Energy Policy.

IEA statistics. 2014. World energy statistics and balances. International Energy Agency (IEA).

Kalyanasundaram, S., E.K. Chong, and N.B. Shroff. 2002. Optimal resource allocation in multi-class networks with user-specified utility functions. *Computer Networks* 38(5): 613-630.

Kenisarin, M., and K. Mahkamov. 2007. Solar energy storage using phase change materials. *Renewable and Sustainable Energy Reviews* 11:1913–1965.

Kolokotsa, D., D. Rovas, E. Kosmatopoulos, and K. Kalaitzakis. 2011. A roadmap towards intelligent net zero- and positive-energy buildings. *Solar Energy* 85: 3067–3084.

Kuo, W. H., and W. Liao. 2007. Utility-based resource allocation in wireless networks. *IEEE Transactions on Wireless Communications* 6(10): 3600-3606.

Lee, K.H., and J.E. Braun. 2008. Development of methods for determining demand-limiting set-point trajectories in buildings using short-term measurements. *Building and Environment* 43(10):1755–1768.

Ling, T., and C. Poon. 2013. Use of phase change materials for thermal energy storage in concrete: An overview. *Construction and Building Materials* 46:55–62.

Ousksou T.K., T.E. Rhafiki, K.E. Omari, Y. Zeraouli, and Y.L. Guer. 2010. Forced convective heat transfer in supercooled phase-change material suspensions with stochastic crystallization. *International journal of refrigeration* 33:1569–1582.

Oya,T., T. Nomura, N. Okinaka, and T. Akiyama. 2012. Phase change composite based on porous nickel and erythritol. *Applied Thermal Engineering* 40:373–377.

Sharma, A., V.V. Tyagi, C.R. Chen, and D. Buddhi. 2009. Review on thermal energy storage with phase change materials and applications. *Renewable and Sustainable Energy Reviews* 13:318–345.

Sun, Y.J., S.W. Wang, and G.S. Huang. 2010. A demand limiting strategy for maximizing monthly cost savings of commercial buildings. *Energy and Building* 42: 2219–2230.

Tyagi, V.V., S.C. Kaushik, S.K. Tyagi, and T. Akiyama. 2011. Development of phase change materials based microencapsulated technology for buildings: a review. *Renewable and Sustainable Energy Reviews* 15:1373–1391.

Varian, H. R. 1992. Microeconomic analysis. W.W. Norton, New York.

Wang, S.W. 1998. Dynamic simulation of a building central chilling system and evaluation of EMCS on-line control strategies. *Building and Environment* 33(1):1-20.

Wang, S.W., X. Xue, and C.C. Yan. 2014. Building power demand response methods toward smart grid. *HVAC&R Research* 20(6):665-687.

Xu, P., and P. Haves. 2006. Case study of demand shifting with thermal mass in two large commercial buildings. *ASHRAE Transactions* 112(1): 572–80.

Xue, X., S.W. Wang, C.C. Yan, and B.R. Cui. 2015. A fast chiller power demand response control strategy for buildings connected to smart grid. *Applied Energy* 137:77-87.

Yuan, J.H., and Z.G. Hu. 2011. Low carbon electricity development in China – an IRSP perspective based on super smart grid. *Renewable and Sustainable Energy Reviews* 15(6):2707–13.

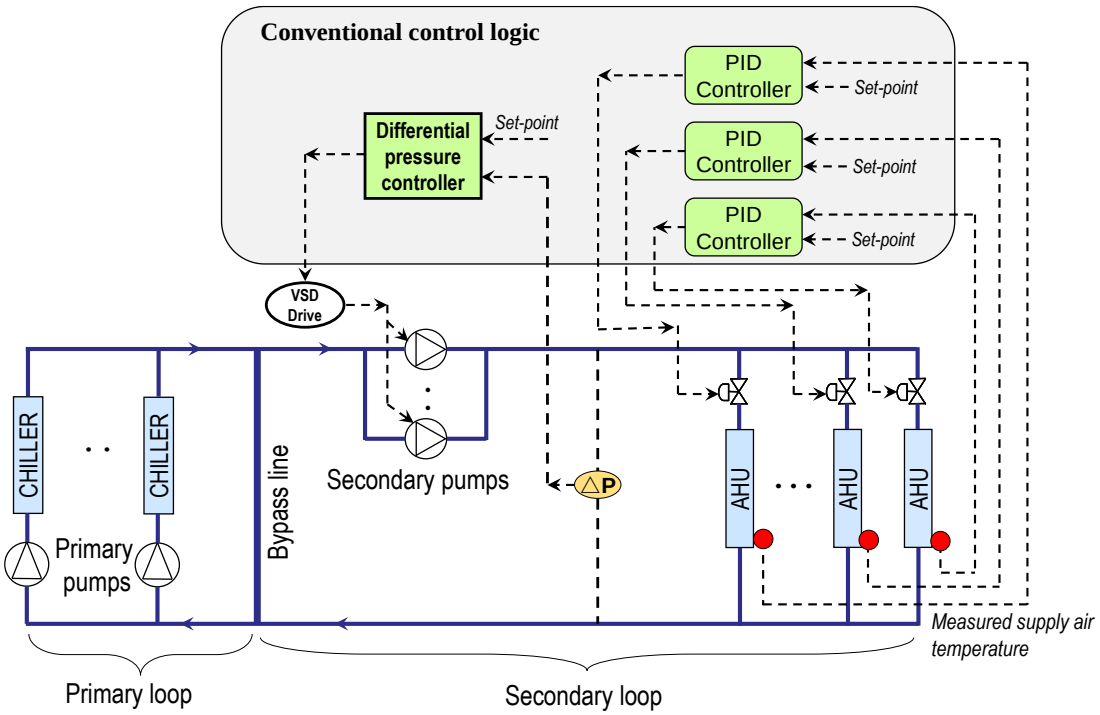

Figure 1. Outline of a typical chilled water system control strategy used today

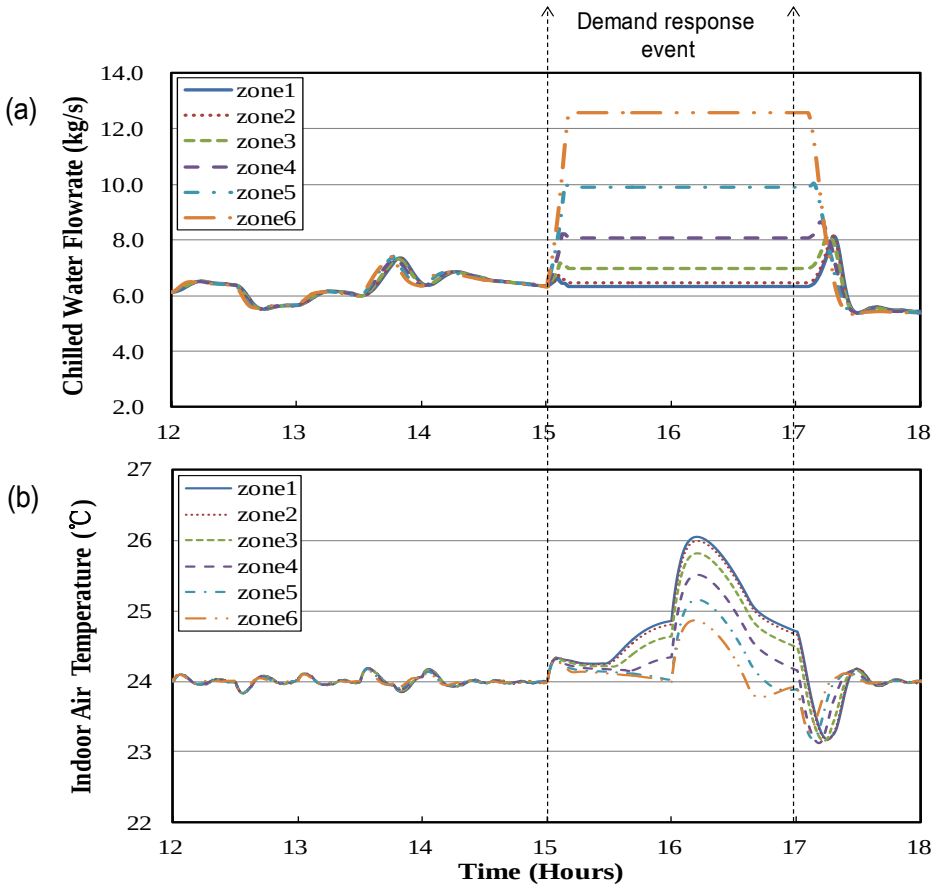

Figure 2. Water distribution and indoor air temperature profiles of a DR test using conventional control strategy

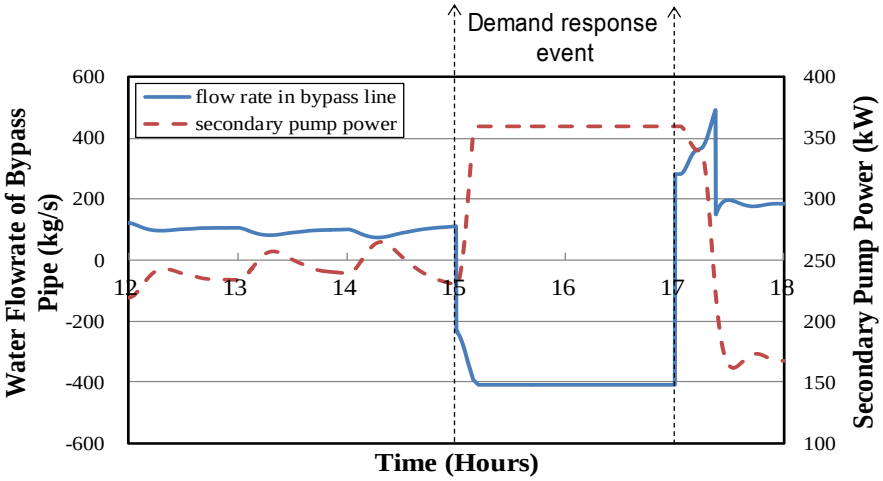

Figure 3. Water flow rate in bypass line and secondary pump power of a DR test using conventional control strategy

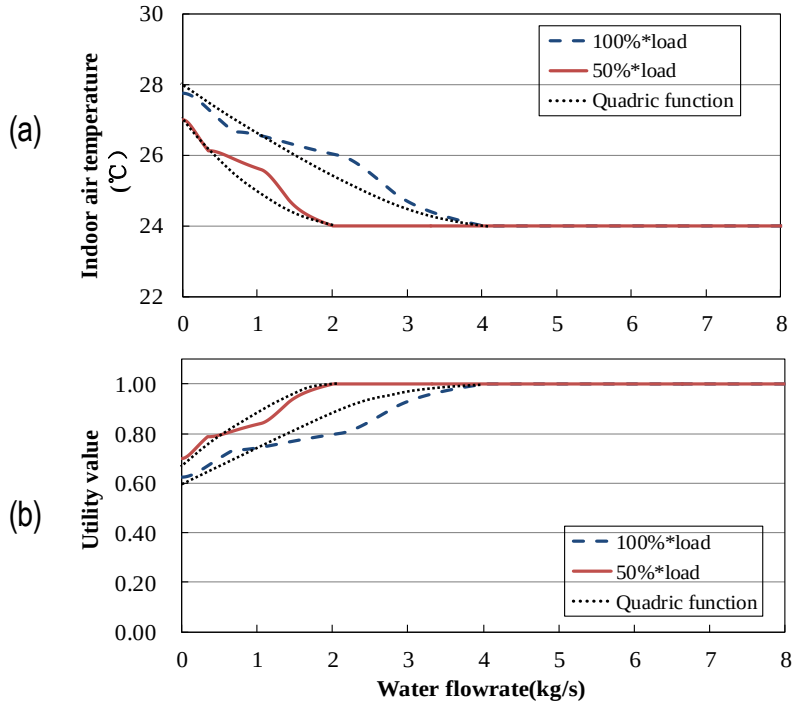

Figure 4. Utility value *vs* chilled water flow rate

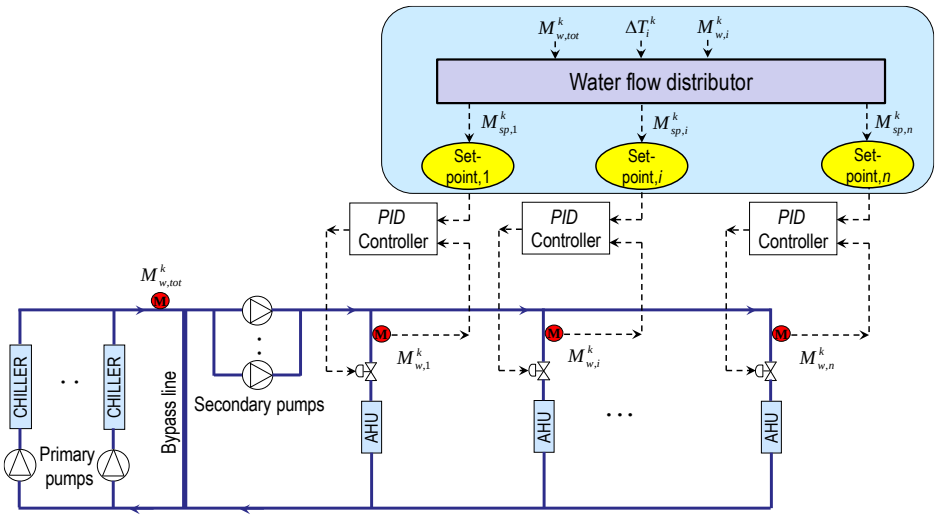

Figure 5. Proposed chilled water flow control strategy

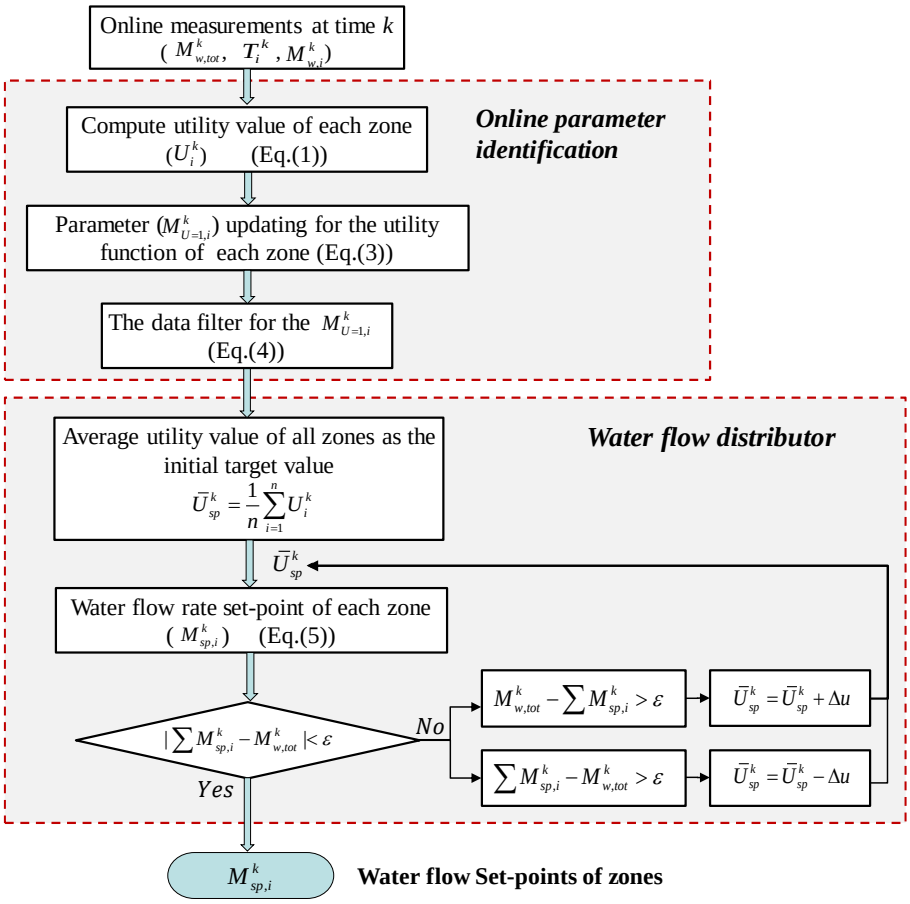

Figure 6. Flow chart for online water flow set-point reset scheme

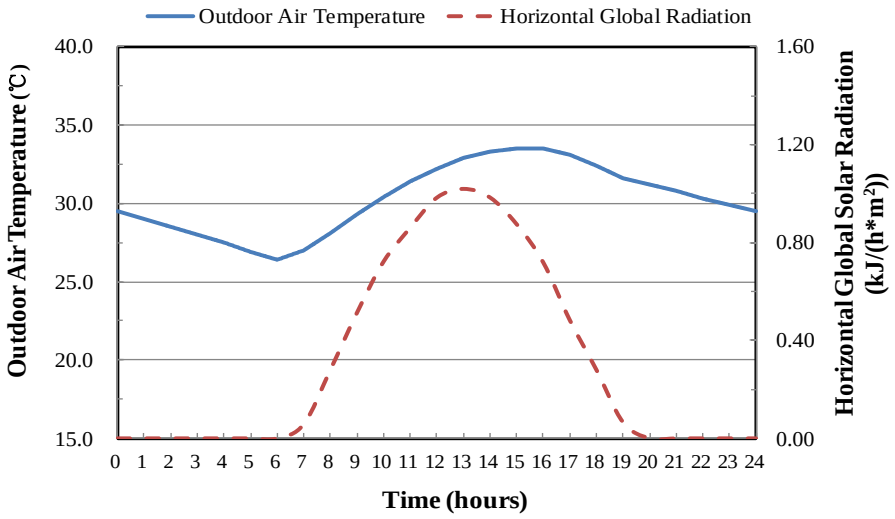

Figure 7. Weather condition of the test day

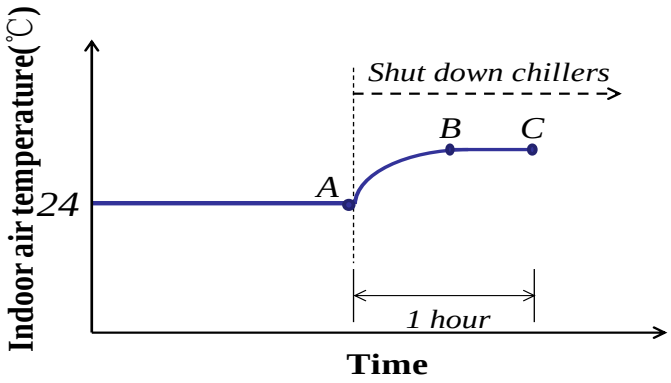

Figure 8. The method of identifying parameter *a*

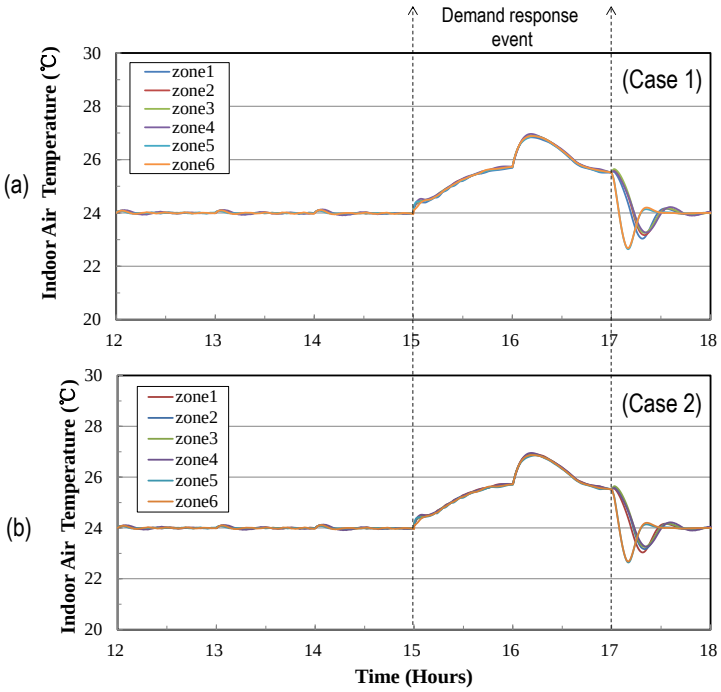

Figure 9. Indoor temperature profiles of two case studies using different values of *a*

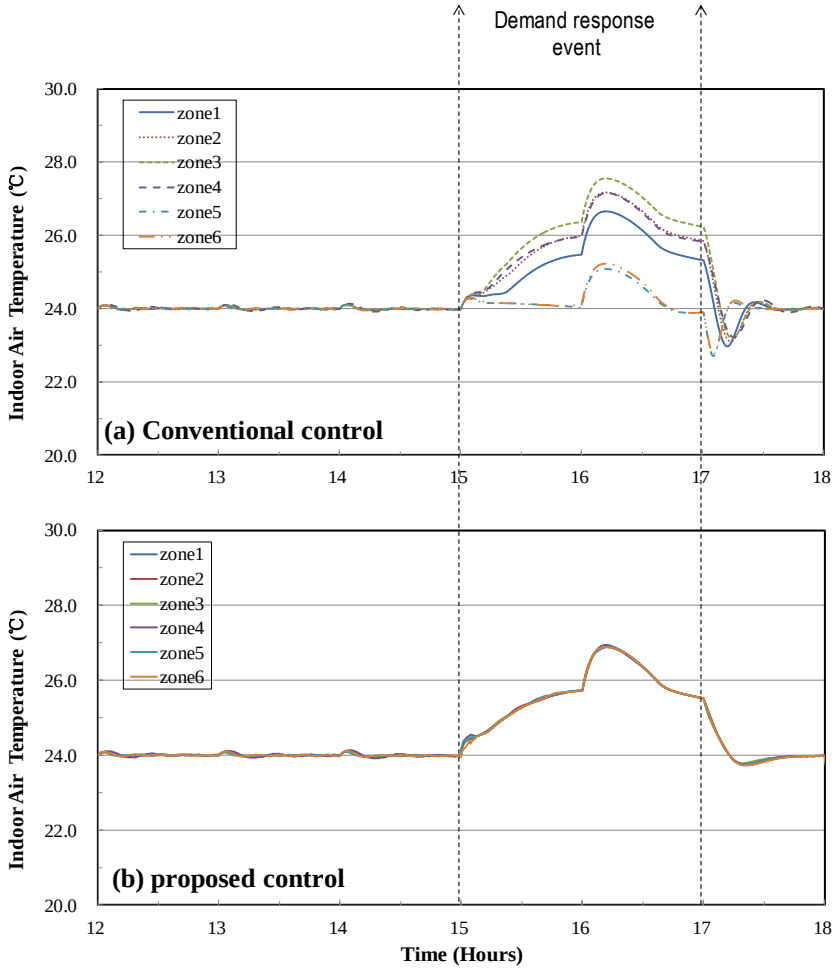

Figure 10. Indoor air temperature profiles of zones in DR tests using conventional control strategy and proposed strategy

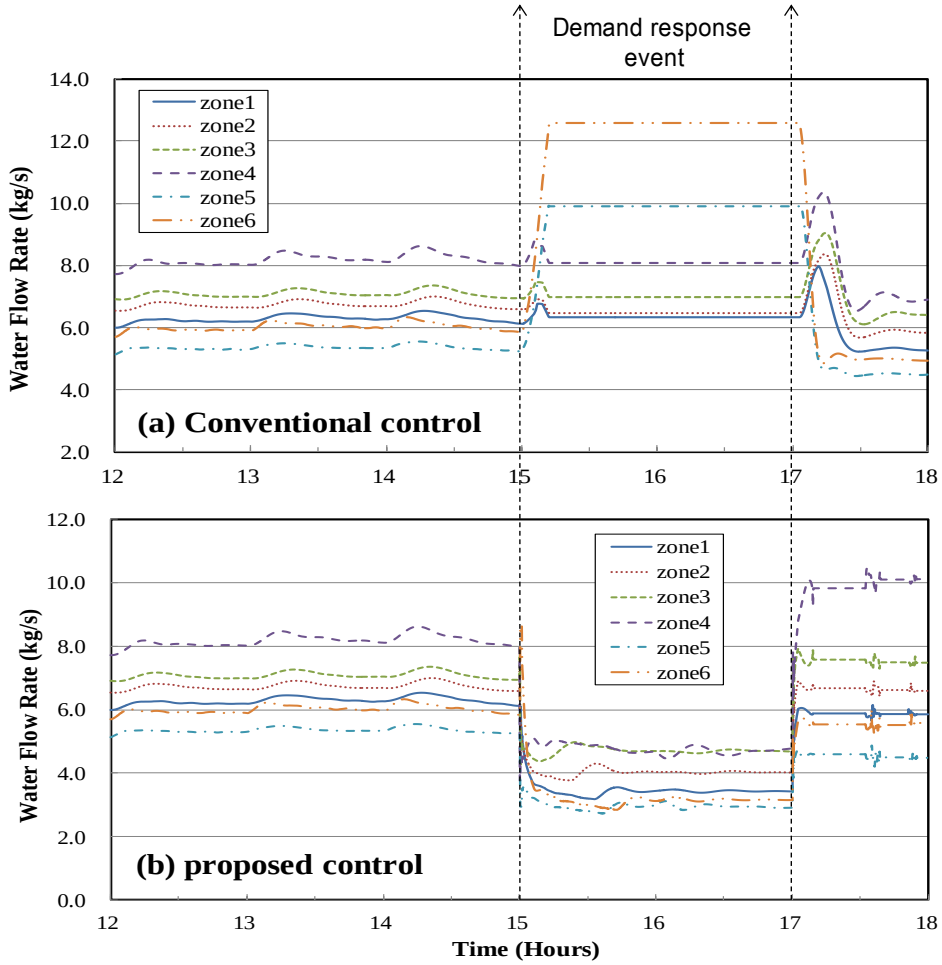

Figure 11. Water flow profiles of zones in DR tests using conventional control strategy and proposed strategy

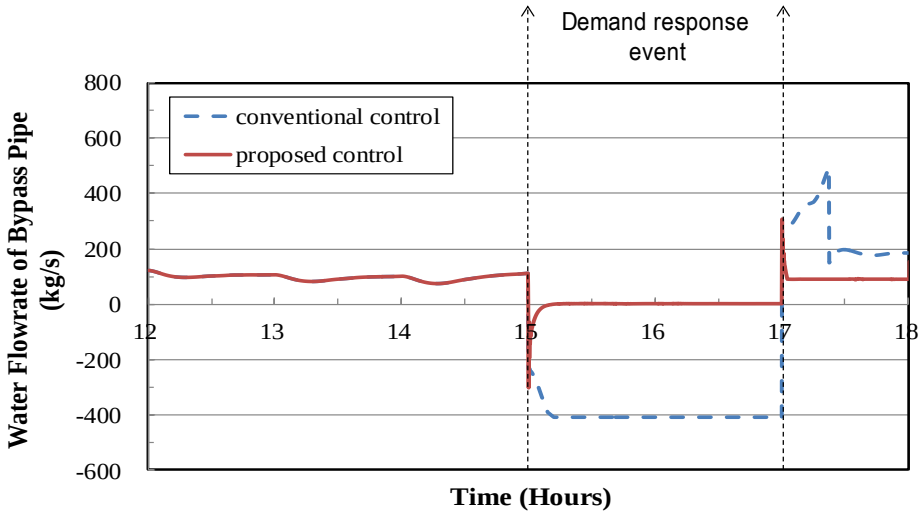

Figure 12. Water flow rates in by-pass line profiles in DR tests using conventional control strategy and proposed strategy

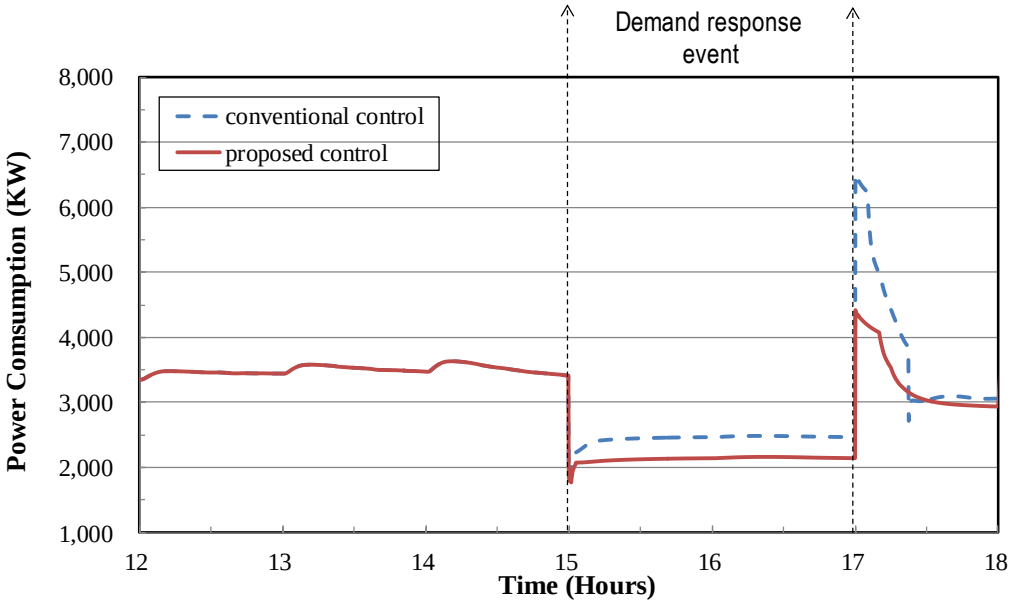

Figure 13. Power consumptions of chillers and chilled water pumps in DR tests using conventional control strategy and proposed strategy

Table 1 The results of parameter a

	Summer case					Mild-summer case				
	Mon.	Tues.	Wed.	Thurs.	Fri.	Mon.	Tues.	Wed.	Thurs.	Fri.
Morning	0.033	0.040	0.031	0.043	0.042	0.044	0.044	0.038	0.036	0.039
Afternoon	0.035	0.034	0.023	0.036	0.038	0.042	0.045	0.038	0.037	0.040

Table 2 The results of parameter a of six zones

	Scale	Average
Zone1	[0.023,0.045]	0.036
Zone2	[0.032,0.046]	0.035
Zone3	[0.031,0.045]	0.034
Zone4	[0.018,0.026]	0.022
Zone5	[0.050,0.065]	0.057
Zone6	[0.034,0.046]	0.041

Table 3 The selected values of parameter a

	Parameter a	
	Zone 1	Other zones
Case 1	0.045	Average value
Case 2	0.023	Average value